Optimal Dispatch Model for Hybrid Energy Storage in Low-Carbon Integrated Energy Systems

Zhe Chen , Pingcheng Cen , Jingbo Zhao , Haixin Wu , Zhixin Fu * , Hao Wang

Posted Date: 25 September 2025

doi: 10.20944/preprints202509.2162.v1

Keywords: Integrated Energy System (IES); Hybrid storage; Low-carbon economic dispatch; Carbon trading mechanism; Independent management of energy storage

 doi:10.20944/preprints202509.2162.v1

Article

Optimal Dispatch Model for Hybrid Energy Storage in Low-Carbon Integrated Energy Systems

Zhe Chen [1], Pingcheng Cen [1], Jingbo Zhao [1], Haixin Wu [2], Hao Wang [2] and Zhixin Fu [2,*]

[1] State Grid Jiangsu Electric Power Co., Ltd. Research Institute.

[2] School of Electrical and Power Engineering, Hoai University, Nanjing, Jiangsu 211100, China

* Correspondence: zhixinfu@hhu.edu.cn; Tel.: +86 18921408723

Abstract

Integrated Energy Systems (IES), which leverage the synergistic coordination of electricity, heat, and gas networks, serve as crucial enablers for a low-carbon transition. Current research predominantly treats energy storage as a subordinate resource in dispatch schemes, failing to simultaneously optimise IES economic efficiency and storage operators' profit maximisation, thereby overlooking their potential value as independent market entities. To address these limitations, this study establishes an operator-autonomous management framework incorporating electrical, thermal, and hydrogen storage in IES. We propose a joint optimal dispatch model for hybrid energy storage systems in low-carbon IES operation. The upper-level model minimises total system operation costs for IES operators, while the lower-level model maximises net profits for independent storage operators managing various storage assets. These two levels are interconnected through power, price, and carbon signals. The effectiveness of the proposed model is verified by setting up multiple scenarios for example analysis.

Keywords: Integrated Energy System (IES); hybrid storage; low-carbon economic dispatch; carbon trading mechanism; independent management of energy storage

1. Introduction

Integrated Energy Systems (IES) deployed at the park level, through the coupling of multiple energy carriers such as electricity, heat, gas, and hydrogen, can significantly improve both the penetration of renewable energy and the overall energy utilisation efficiency. As such, IES serve as a key enabler in the transition toward clean and low-carbon energy systems[1].

In recent years, extensive research has been conducted on various technologies aimed at promoting low-carbon IES operation, including Demand Response (DR), tiered carbon trading mechanisms, Carbon Capture and Storage (CCS), and Power-to-Gas (P2G) strategies[2–4]. These approaches have all contributed—albeit to varying extents—to enhancing renewable energy integration and reducing carbon emissions within IES. However, a critical challenge remains: how to achieve low-carbon objectives while simultaneously ensuring economic viability and operational flexibility of the system. This trade-off remains a central focus of current research efforts.

As a crucial component of IES, energy storage plays a central role in ensuring stable system operation and enhancing both economic performance and operational flexibility, primarily through peak shaving and energy shifting mechanisms[5]. Among various storage technologies, electrical energy storage (EES) is the most widely adopted in IES, and most existing studies have focused on the optimal dispatch of EES systems. For instance, [6] proposed a multi-objective bi-level optimal model incorporating energy storage to improve system economics, stability, and environmental sustainability. In [7], storage planning was extended beyond electricity to include multiple energy forms within IES, namely, electricity, heat, and gas. The authors designed the capacity configuration of both electrical and thermal storage systems from the perspective of achieving system-wide economic optimality.

 doi:10.20944/preprints202509.2162.v1

However, conventional electrochemical storage technologies are often limited by their energy density and discharge duration, making them less suitable for high-capacity and long-duration applications. In contrast, hydrogen energy storage (HES) offers advantages such as large capacity, long storage duration, and clean energy characteristics [8]. Furthermore, the synergistic coupling of hydrogen with electricity and heat enables efficient coordination across energy carriers, thereby delivering cost-effective, large-scale, long-duration regulation. This not only facilitates the integration of renewable energy but also effectively mitigates fluctuations in electricity and thermal systems [9]. Consequently, growing attention has been paid to the role of hydrogen storage in IES. For example, [10] developed an IES model comprising wind turbines, gas turbines, hydrogen power units, and hydrogen storage systems, and demonstrated that the incorporation of hydrogen storage significantly reduced wind curtailment and enhanced renewable energy utilization. In [11] , an optimal method was proposed for the configuration of an integrated electricity-heat-gas-hydrogen energy system, considering tiered carbon trading and seasonal hydrogen storage. The model effectively addressed the seasonal mismatch between renewable energy output and load demand, while also considering economic and low-carbon performance objectives.

Most of the aforementioned studies primarily focus on the optimal scheduling of either EES or HES. However, given that IES inherently operate as multi-energy coupled systems, involving electricity, heat, and gas, relying solely on a single type of storage is insufficient to fully exploit the system's flexibility and low-carbon potential. As a result, the coordinated optimisation of multiple storage types has emerged as a new research focus. For instance,[12] proposed a hybrid renewable energy system combining hydrogen storage and battery systems and utilised advanced algorithms to optimise overall system performance. In [13] , a multi-energy storage capacity allocation model was developed to provide various load-shifting strategies, thereby reducing system load fluctuations and enhancing the reliability of the storage system. Furthermore, [14] constructed a bi-level economic optimal model that considers natural gas-hydrogen blending alongside the coordinated operation of multiple types of energy storage. This approach promotes flexible interaction among electrical, thermal, and hydrogen storage systems, thus enhancing multi-energy complementarity within the IES framework.

Although the aforementioned studies have expanded the application of multi-type energy storage systems within IES, most still treat storage as a subordinate component within the overall IES optimal framework, making it difficult to realise its potential value as an independent market participant. In practice, the integrated planning and dispatch of storage with IES can impose significant investment pressure on the system. Moreover, under a multi-objective environment that includes both carbon trading and demand response (DR), the profit margin of storage systems may be compressed, making it challenging to simultaneously achieve both economic and low-carbon benefits. Against this backdrop, a number of recent studies have begun to explore models in which energy storage participates in IES optimisation as an independent operator. For example, [15] introduced a distributed robust optimal approach to conduct a comprehensive quantitative evaluation of hydrogen storage systems, and proposed a framework to assess their multi-dimensional value, thereby providing methodological support for independent storage operation.

In summary, this paper proposes a bi-level optimal model for the independent scheduling of HES, under the overarching goal of enabling low-carbon operation in IES. The model decouples electrical, thermal, and hydrogen energy storage from the internal structure of the IES and treats them as independent market entities with autonomous decision-making capabilities. The proposed hybrid storage configuration model consists of two hierarchical levels: The upper-level model, governed by the IES operator, aims to minimise the total system operating cost, considering factors such as energy procurement, carbon trading, renewable curtailment penalties, CCS costs, and DR compensation. The lower-level model, led by independent storage operators, aims to maximise net profit by evaluating investment returns and market price signals (electricity, heat, etc.), thereby enabling profit-driven decision-making by storage service providers. The interaction between the two layers is mediated through price and energy signals, forming a bi-level optimal framework with Stackelberg game

 doi:10.20944/preprints202509.2162.v1

characteristics. This structure facilitates efficient coordination between system-wide low-carbon objectives and localised profitability targets.

The key advantages of the proposed model include:

(1) Integrated market-based regulation: By incorporating electricity prices, carbon prices, and emission quotas into a unified market mechanism, the model synergistically embeds DR, CCS, carbon trading, and energy storage optimisation. This enables coordinated decarbonization, cost reduction, and flexibility enhancement through market-driven incentives.

(2) Independent market roles for multi-energy storage: By assigning autonomous market roles to electrical, thermal, and hydrogen storage units, the model leverages temporal arbitrage and load reshaping to enhance local renewable energy consumption. This supports the system-level coordination of low-carbon operation, economic efficiency, and operational flexibility.

2. Framework for Low-Carbon Coordinated Operation of IES Integrating Generation, Grid, Load, and Storage

2.1 IES System Architecture

As a crucial platform for multi-energy coordinated optimisation, the IES facilitates complementary energy supply by coupling various energy carriers, including electricity, heat, gas, and hydrogen. The low-carbon coupled operation framework constructed in this paper incorporates wind power, photovoltaics, Thermal Power Units (TPUs), Combined Heat and Power (CHP) units, Gas Boilers (GBs), Electric Boilers (EBs), Carbon Capture Systems (CCS) and Power-to-Gas (P2G) technology, along with three types of energy storage: electrical, thermal, and hydrogen. Through energy coupling, this system achieves multi-energy complementarity and flexible regulation, with its architecture illustrated in Figure 1.

When renewable energy generation within the IES exceeds local electrical demand, the surplus power is preferentially routed by the storage operator to the electrical storage system, while a portion is converted into hydrogen via an electrolyser and stored in a hydrogen tank. During periods of high electricity prices or high system marginal costs, the stored hydrogen is supplied to a fuel cell to generate power, thereby replacing high-priced purchased electricity and enabling inter-temporal price arbitrage. Concurrently, waste heat from both the electrolysis and fuel cell processes is recovered and stored in a thermal storage tank. This stored heat supplements the supply during peak thermal loads or when conventional heating sources (e.g., gas boilers) are insufficient, thus enhancing overall energy efficiency and supply continuity. Through this integrated operation, the operational value of energy storage as an independent market entity is fully realised.

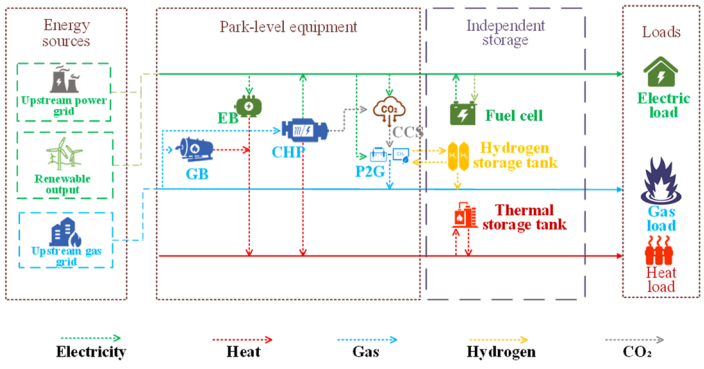

Figure 1. IES system architecture

2.2 Low-Carbon Coupled Operation Mechanism and Model for IES Integrating Generation, Grid, Load, and Storage

 doi:10.20944/preprints202509.2162.v1

2.2.1 Low-Carbon Coupled Operation Mechanism for IES Integrating Generation, Grid, Load, and Storage

To enhance the system's low-carbon performance and emission reduction effectiveness while ensuring flexibility and sustainability, this study introduces several low-carbon operational mechanisms across the generation, grid, load, and storage domains, as illustrated in Fig.2.

On the generation side, A tiered carbon trading mechanism is implemented to incentivise the reduction of high-carbon energy consumption. This is combined with a post-combustion CCS featuring flue gas splitting to enable flexible capture regulation. Furthermore, a two-stage P2G process absorbs surplus renewable electricity and synergistically utilises CO_2 with the CCS, thereby enhancing low-carbon and flexible supply capabilities.

On the network side: The multi-energy grid (electricity, heat, gas, hydrogen) leverages interactions with energy storage and P2G. At the physical level, this facilitates cross-media energy conversion and peak-valley shifting. At the economic level, a unified carbon price, combined with various energy market prices (for electricity, heat, and gas), forms a tripartite signalling channel of cost, energy, and carbon to optimise power flow and energy distribution.

On the load side, the transferability and substitutability of DR are utilised to reshape the energy consumption curve. Driven by price and carbon signals, demand is shifted across time periods and energy carriers, coordinating with flexible generation to enhance local renewable energy consumption and reduce energy use during high-carbon intervals.

On the storage side: Multiple storage types (electrical, thermal, and hydrogen) are treated as independent, tradable entities. They perform multiple functions, including energy time-shifting, capacity support, provision of reserves, and ramp mitigation. These entities participate in the market across three dimensions, i.e., energy, ancillary services, and carbon reduction revenue, to achieve synergistic gains in both economic efficiency and low-carbon performance.

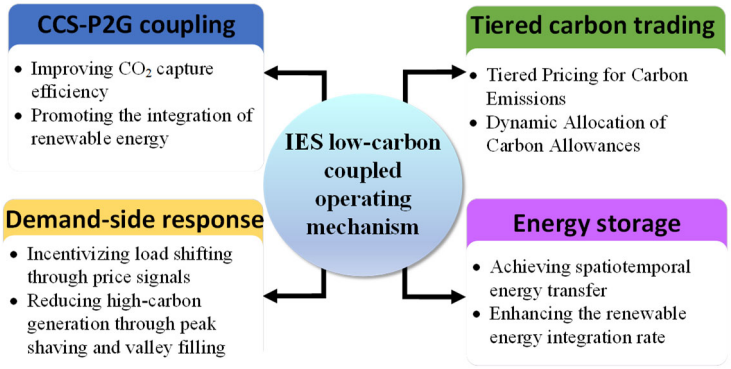

Figure 2. IES low-carbon coupled operating mechanism

2.2.2 Model of the IES Low-Carbon Coupled Operation Mechanism

The objective of this study is to achieve a low-carbon economic operation of IES through the optimal dispatch of hybrid electrical, thermal, and hydrogen storage. For the sake of brevity, the models for fundamental equipment, including electrical supply units (wind turbines, photovoltaics, TPUs, and CHP units) and thermal supply units (CHP, GBs, and EBs), are referenced from [16] and will not be reiterated here. Building upon the framework illustrated in Fig.2, the following sections will present the models for the key equipment integral to the low-carbon coupled operation mechanism.

1. Carbon Capture System Model

By integrating post-combustion capture methods with flue gas splitting technology and incorporating a dedicated CO_2 storage tank, this study develops a flue gas splitting-based CCS. This configuration enables flexible regulation of both the carbon capture volume and the system's overall energy consumption. The corresponding mathematical model is presented in Equation (2.1) [17]:

 doi:10.20944/preprints202509.2162.v1

$$\begin{cases} P_t^{CCS} = e_c E_t^r \\ P_t^{CCS,total} = P_t^{CCS} + P^B \\ E_t^a = E_t - e_t^a \\ 0 \le P_t^{CCS} \le P_{max}^{CCS} \end{cases} \quad (1)$$

where $P_t^{CCS,total}$ is the total energy consumption of the CCS system; P_t^{CCS} is the operating energy consumption incurred during capture; P^B is the fixed baseline energy consumption of the CCS; e_c is the specific energy consumption required to capture a unit mass of CO_2; E_t^a is the amount of CO_2 captured by the CCS at time t; E_t is the total CO_2 emitted by the unit; P_{max}^{CCS} is the upper bound on CCS operating energy consumption; e_t^a is the amount of CO_2 directly vented to the atmosphere via the flue-gas bypass at time t.

The solvent storage unit within the CCS is composed of a lean solution tank and a rich solution tank. Adjusting the solution levels in these tanks enables the temporal decoupling of the CO2 absorption and solvent regeneration processes. The mathematical model for these storage tanks is presented in Equation (2.2):

$$\begin{cases} V_t^R = V_{t-1}^R + v_t^{R,in} - v_t^{R,out} \\ V_t^L = V_{t-1}^L + v_t^{L,in} - v_t^{L,out} \\ v_t^{R,out} = v_t^{L,in} \\ v_t^{L,out} = v_t^{R,in} \end{cases} \quad (2)$$

where V_t^R is the volume of rich solvent at time t ; V_t^L is the volume of lean solvent at time t; $v_t^{R,in}$ and $v_t^{R,out}$ are the inflow to and outflow from the rich-solution tank, respectively; $v_t^{L,in}$ and $v_t^{L,out}$ are the inflow and outflow from the lean-solution tank, respectively.

2. Two-Stage P2G Model

To fully leverage the low-carbon benefits of hydrogen, the P2G process is disaggregated into two distinct stages: water electrolysis and methanation. The specific mathematical model for the water electrolysis process is as follows:

Water Electrolysis Process:

$$\begin{cases} P_t^{EW,H_2} = \eta^{EW} P_t^{e,EW} \\ P_{min}^{e,EW} \le P_t^{e,EW} \le P_{max}^{e,EW} \\ \Delta P_{min}^{e,EW} \le P_{t+1}^{e,EW} - P_t^{e,EW} \le \Delta P_{max}^{e,EW} \end{cases} \quad (3)$$

where $P_t^{e,EW}$ is the electrical energy input to the electrolytic tank at time t; P_t^{EW,H_2} is the hydrogen energy output from the electrolytic tank at time t; η^{EW} is the energy-conversion efficiency; $P_{min}^{e,EW}$ and $P_{max}^{e,EW}$ are the lower and upper bounds of the electrolytic tank's input electrical power; $\Delta P_{min}^{e,EW}$ and $\Delta P_{max}^{e,EW}$ are the downward and upward ramping limits of the electrolytic tank, respectively.

Methanation stage:

$$\begin{cases} P_t^{MR,g} = \eta^{MR} P_t^{H_2,MR} \\ P_{min}^{H_2,MR} \le P_t^{H_2,MR} \le P_{max}^{H_2,MR} \\ \Delta P_{min}^{H_2,MR} \le P_{t+1}^{H_2,MR} - P_t^{H_2,MR} \le \Delta P_{max}^{H_2,MR} \end{cases} \quad (4)$$

where $P_t^{MR,g}$ and $P_t^{H_2,MR}$ are the methane output power and the hydrogen input power of the methanation unit at time t, respectively; $P_{min}^{H_2,MR}$ and $P_{max}^{H_2,MR}$ are the lower and upper bounds of the methanation unit's output; $\Delta P_{min}^{H_2,MR}$ and $\Delta P_{max}^{H_2,MR}$ are the downward and upward ramp-rate limits of the methanation unit.

3. Tiered Carbon Trading Model

In IES dispatch models guided solely by the minimisation of fuel or energy procurement costs, the externality of carbon emissions is often not effectively internalised. This leads to a dispatch strategy that favours high-carbon generation sources, such as coal-fired units and gas boilers. Concurrently, renewable energy sources are subject to curtailment due to their inherent volatility, while energy storage and demand response lack effective price signals to incentivise their operation. As a result, the system struggles to reconcile economic efficiency with emission reduction targets. Therefore, this paper introduces a tiered carbon trading model to make the carbon constraint explicit

 doi:10.20944/preprints202509.2162.v1

and strengthen the economic incentive for emission abatement by applying progressively higher marginal carbon prices to different tiers of excess emissions [18].

The tiered carbon trading mechanism partitions the total required carbon allowances into multiple purchasing intervals. As the volume of purchased allowances increases, the corresponding marginal price for each successive tier becomes higher. The mathematical formulation for the tiered carbon trading model is as follows:

$$C_{CO_2} = \begin{cases} \lambda E_{\mathrm{IES,t}}, E_{\mathrm{IES,t}} \le l \\ \lambda(1+\alpha)(E_{\mathrm{IES,t}} - l) + \lambda l, l < E_{\mathrm{IES,t}} \le 2l \\ \lambda(1+2\alpha)(E_{\mathrm{IES,t}} - 2l) + (2+\alpha)\lambda l, 2l < E_{\mathrm{IES,t}} \le 3l \\ \lambda(1+3\alpha)(E_{\mathrm{IES,t}} - 3l) + (3+3\alpha)\lambda l, 3l < E_{\mathrm{IES,t}} \le 4l \\ \lambda(1+4\alpha)(E_{\mathrm{IES,t}} - 4l) + (4+6\alpha)\lambda l, 4l < E_{\mathrm{IES,t}} \end{cases} \tag{5}$$

here $E_{\mathrm{IES,t}}$ is the quantity of carbon allowances traded by the IES at time t; $C_{\mathrm{CO_2}}$ is the carbon-trading cost; λ is the base carbon-trading price; l is the length of the emissions interval; α is the price escalation rate.

4. Demand Response Model

DR utilises joint signals and incentives, such as electricity, heat, gas, and carbon prices, to encourage users to autonomously adjust their energy consumption without compromising service quality or comfort, thereby enhancing operational efficiency and reducing carbon intensity. The IES constructed in this paper aggregates multiple types of dispatchable resources, where electricity, heat, and gas loads can undergo both cross-temporal shifting (for peak shaving and valley filling) and cross-carrier substitution within the same time period (e.g., substituting gas-fired heating with electric heating).

In the proposed model, DR operates in synergy with energy storage, P2G, and CCS to reshape the load profile. This coordination aims to increase local renewable energy consumption, suppress the dispatch of high-carbon marginal units, and lower the overall system carbon intensity. Following the methodology in reference [19], the total load is classified into fixed, shiftable, and substitutable types. The value of load type k at time period t is denoted as:

$$P_{\mathrm{k,Load}}(t) = P^{\mathrm{s,0}}_{\mathrm{k,Load}}(t) + P^{\mathrm{p,0}}_{\mathrm{k,Load}}(t) + P^{\mathrm{c,0}}_{\mathrm{k,Load}}(t) \tag{6}$$

where $k \in \{\mathrm{e,h,g}\}$ is the energy carrier: electricity (e), heat (h), and gas (g). $P_{\mathrm{k,Load}}(t)$ is the value of the k-type load at time t; $P^{\mathrm{s,0}}_{\mathrm{k,Load}}(t)$ is the fixed component; $P^{\mathrm{p,0}}_{\mathrm{k,Load}}(t)$ is the shiftable component; and $P^{\mathrm{c,0}}_{\mathrm{k,Load}}(t)$ is the substitutable component.

3 Optimal Dispatch Model of Hybrid Storage in an IES with an Independent Storage Operator

To reflect the independent operational nature of energy storage systems, this paper constructs a bilevel optimal framework with Stackelberg characteristics: the upper level addresses the coordinated dispatch problem for the IES operator, aiming to minimise the total system operating cost, while the lower level deals with the operational capacity configuration of the independent energy storage operator, targeting net profit maximisation. The bilevel optimal logic is illustrated in Figure 3, with the two levels coupled through two types of quantities: one is physical coupling quantities, primarily including the flow and exchange of four energy types- electricity, heat, gas, and hydrogen- as well as power constraints of related equipment in the IES. These quantities are involved in both the upper-level electricity-heat-gas-hydrogen balance and network constraints and determine the lower-level settlement electricity volumes and cost/revenue calculations. The other is environmental signalling quantities, including electricity, heat, and gas prices, carbon quotas, and forecasts of load and renewable energy output. These are passed down from the upper to the lower level, driving the optimal response of energy storage. To improve the efficiency of model solving, this paper employs the strong duality KKT conditions to embed the lower-level optimality into the upper level, forming an equivalent single-level MILP model for unified solution.

 doi:10.20944/preprints202509.2162.v1

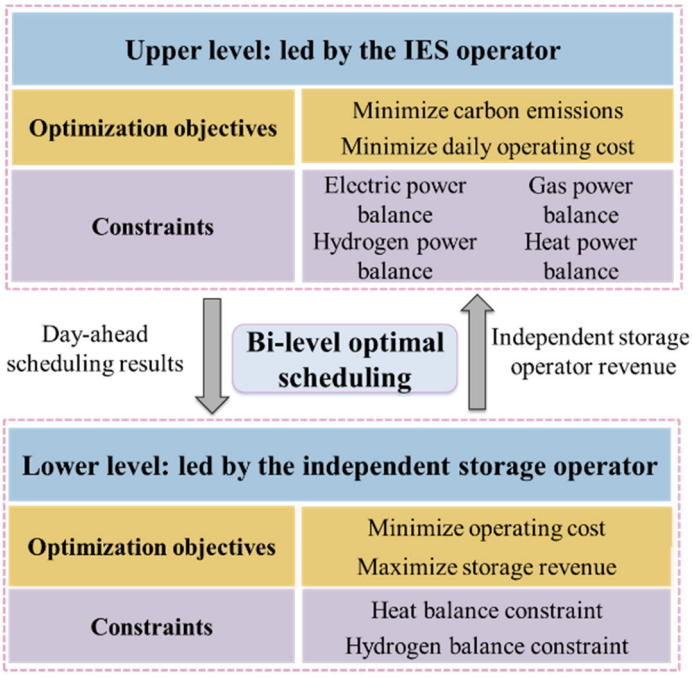

Figure 3. Bi-level optimal logic diagram

3.1 Upper-Level Low-Carbon Operation Model for the IES

The upper-level objective function aims to minimise the total operating cost of the IES system while incorporating multiple cost components, including energy procurement, tiered carbon trading, wind/solar curtailment, CCS, and DR compensation. This approach enables unified consideration of carbon constraints and economic objectives within a single framework, demonstrating greater comprehensiveness compared to traditional models that only account for energy procurement or single environmental costs.

Regarding low-carbon mechanism integration, the model embeds the operational principles of flue gas split-flow CCS, two-stage P2G and DR into upper-level decision-making and constraints. This not only enhances local renewable energy consumption capacity but also provides institutionalised interfaces for synergies among different low-carbon measures.

Furthermore, through triple-signal coupling ("price-energy-carbon") with lower-level entities, the upper level can transmit carbon costs, energy margins, and price expectations downward, thereby guiding hybrid energy storage systems to make optimal responses aligned with overall system objectives.

3.1.1 Objective Function

The specific objective is:

$$F\_\text{upper} = \min(C_{\text{buy}} + C_{\text{CO}_2} + C_{\text{DG,cut}} + C_{\text{CCS}} + C_{\text{DR}}) \tag{1}$$

The energy-procurement cost C_{buy} is:

$$C_{\text{buy}} = \sum_{t=1}^{T} \alpha_t P_{\text{e,buy}}(t) + \sum_{t=1}^{T} \beta_t P_{\text{g,buy}}(t) \tag{2}$$

where $P_{\text{e,buy}}(t)$ represents the electricity purchased by the IES during time period t; $P_{\text{g,buy}}(t)$ denotes the natural gas purchased by the IES during time period t; α_t and β_t are the electricity price and natural gas price at time t, respectively.

The calculation method for carbon trading cost C_{CO_2} is detailed in the Equation (5).

Curtailment cost C_{cut} is:

 doi:10.20944/preprints202509.2162.v1

$$C_{\text{cut}} = \delta_{\text{DG}} \sum_{t=1}^{T} P_{\text{DG,cut}}(t) + \delta_{\text{PV}} \sum_{t=1}^{T} P_{\text{PV,cut}}(t) \tag{3}$$

where δ_{DG} and δ_{PV} represent the penalty costs per unit of curtailed wind and photovoltaic power, respectively; $P_{\text{DG,cut}}(t)$ and $P_{\text{PV,cut}}(t)$ denote the curtailed wind power and photovoltaic power at time t, respectively.

The carbon sequestration cost C_{CCS} is calculated as:

$$C_{\text{CCS}} = c_{\text{CCS}} \sum_{t=1}^{T} E_{\text{t}}^{\text{a}}(t) \tag{4}$$

where c_{CCS} denotes the carbon sequestration cost coefficient; $E_{\text{t}}^{\text{a}}(t)$ represents the CO_2 mass captured by the CCS system at time t.

The demand response (DR) compensation cost C_{DR} is given by:

$$C_{\text{DR}} = \sum_{k=1}^{3} \sum_{t=1}^{T} (\delta_{\text{p}} \mid \Delta P_{\text{k,Load}}^{\text{p}}(t) \mid + \delta_{\text{c}} \mid \Delta P_{\text{k,Load}}^{\text{c}}(t) \mid) \tag{5}$$

where δ_{p} and δ_{c} represent the unit compensation coefficients for shiftable loads and substitutable loads participating in demand response (DR), respectively.

3.1.2 Constraints

Power-balance constraints

The constraints primarily include power balance equations for four energy carriers: electricity, heat, gas, and hydrogen, as formulated below:

$$\begin{aligned} &P_{\text{t}}^{\text{e,buy}} + P_{\text{t}}^{\text{EM}} + P_{\text{t}}^{\text{pv}} + P_{\text{t}}^{\text{wind}} + P_{\text{t}}^{\text{E,dis}} + P_{\text{t}}^{\text{CHP}} = \\ &P_{\text{t}}^{\text{e,EW}} + P_{\text{t}}^{\text{EB}} + P_{\text{t}}^{\text{CCS}} + P_{\text{e}}^{\text{load}}(t) + P_{\text{t}}^{\text{E,cha}} \end{aligned} \tag{6}$$

$$H_{\text{t}}^{\text{CHP}} + H_{\text{t}}^{\text{GB}} + H_{\text{t}}^{\text{EB}} + H_{\text{t}}^{\text{hot,dis}} = P_{\text{h}}^{\text{load}}(t) + H_{\text{t}}^{\text{hot,cha}} \tag{7}$$

$$P_{\text{t}}^{\text{grid,g}} + P_{\text{t}}^{\text{MR,g}} = P_{\text{t}}^{\text{CH}_4\text{,CHP}} + P_{\text{t}}^{\text{CH}_4\text{,GB}} + P_{\text{g}}^{\text{load}}(t) \tag{8}$$

$$P_{\text{t}}^{\text{EW,H}_2} + V_{\text{t}}^{\text{H}_2\text{,dis}} = V_{\text{t}}^{\text{H}_2\text{,cha}} + P_{\text{t}}^{\text{H}_2\text{,CHP}} + P_{\text{t}}^{\text{H}_2\text{,GB}} + P_{\text{t}}^{\text{H}_2\text{,MR}} \tag{9}$$

where $P_{\text{t}}^{\text{e,buy}}$ is electricity purchased by the integrated energy system; P_{t}^{EM} is the output of coal-fired generation units; P_{t}^{pv} and $P_{\text{t}}^{\text{wind}}$ are the output of photovoltaic and wind turbine units respectively; $P_{\text{t}}^{\text{CHP}}$ is the electrical output of the CHP unit; $P_{\text{t}}^{\text{E,cha}}$ and $P_{\text{t}}^{\text{E,dis}}$ are the charging and discharging power of the EES; $P_{\text{t}}^{\text{e,EW}}$ is the electric power absorbed by the electrolytic tank; P_{t}^{EB} is the electric power consumed by the electric boiler; $P_{\text{t}}^{\text{CCS}}$ is the electric power consumed by the CCS system; $P_{\text{e}}^{\text{load}}(t)$ is the electric load at time t. $P_{\text{h}}^{\text{load}}(t)$ is the thermal load at time t; $H_{\text{t}}^{\text{hot,cha}}$ and $H_{\text{t}}^{\text{hot,dis}}$ are the charging and discharging thermal power of thermal energy storage system. $P_{\text{t}}^{\text{grid,g}}$ is the amount of gas purchased by the system; $P_{\text{g}}^{\text{load}}$ is the gas load. $P_{\text{t}}^{\text{MR,g}}$ is the CH_4 generated by P2G; $V_{\text{t}}^{\text{H}_2\text{,cha}}$ and $V_{\text{t}}^{\text{H}_2\text{,dis}}$ are the Hydrogen charging and discharging volumes of the HES system.

5. TPUs Output Constraints

$$\begin{cases} P_{\text{min}}^{\text{C}} \le P_{\text{t}}^{\text{C}} \le P_{\text{max}}^{\text{C}} \\ \Delta P_{\text{min}}^{\text{C}} \le P_{\text{t}}^{\text{C}} - P_{\text{t-1}}^{\text{C}} \le \Delta P_{\text{max}}^{\text{C}} \end{cases} \tag{10}$$

where $P_{\text{min}}^{\text{C}}$ and $P_{\text{max}}^{\text{C}}$ represent the lower and upper limits of TPUs output, respectively; $\Delta P_{\text{min}}^{\text{C}}$ and $\Delta P_{\text{max}}^{\text{C}}$ denote the downward and upward ramping limits of the TPUs, respectively.

6. Wind and PV Generation Constraints

$$\begin{cases} p_{\text{t}}^{\text{pv}} = P_{\text{t}}^{\text{pv}} - P_{\text{t}}^{\text{pvc}} \\ 0 \le P_{\text{t}}^{\text{pv}} \le P_{\text{max}}^{\text{pv}} \end{cases} \tag{11}$$

$$\begin{cases} p_{t}^{\text{wind}} = P_{t}^{\text{wind}} - P_{t}^{\text{windc}} \\ 0 \le P_{t}^{\text{wind}} \le P_{\text{max}}^{\text{wind}} \end{cases} \tag{12}$$

 doi:10.20944/preprints202509.2162.v1

where P_t^{PV} and P_{max}^{PV} are the actual photovoltaic output and its upper limit at time t; P_t^{pvc} is the curtailed PV power. Similarly, P_t^{wind} and P_{max}^{wind} are the Actual wind power output and its upper limit at time t; P_t^{windc} is the curtailed wind power.

7. Other constraints

The tiered carbon-trading constraints are given by Equation (5); the DR constraints are formulated in Equation (6). The system also includes other device-level constraints, such as the CCS operational constraints in Equations (1)~(2); The P2G unit constraints in Equations (3)~(4);

3.2 Lower-Level Energy Storage Optimal Dispatch Model

The lower-level energy storage dispatch model decouples electricity, thermal, and hydrogen storage from the IES's centralised ancillary resources as independent operational entities. With the objective of net profit maximisation, the model simultaneously incorporates investment costs and operational revenues (e.g., charging/discharging, heat storage/release, hydrogen production/release) into the objective function, achieving a unified economic characterisation of multiple energy storage types. This approach grants storage systems market-oriented autonomous decision-making authority, fully expanding their value potential and strategic flexibility.

The model establishes operational constraints for electrical, thermal, and hydrogen storage systems based on key parameters, including capacity, power rating, efficiency, self-discharge, and switching states. It meticulously captures cross-temporal energy shifting and efficiency loss mechanisms to ensure engineering feasibility of profit-maximising decisions, while providing independent operators with enhanced arbitrage and dispatch flexibility.

3.2.1 Objective Function

The specific objective function is formulated as:

$$C_{ESS} = C_{in} - C_{cost} \tag{13}$$

where

$$\begin{cases} C_{in} = \eta_r^e \sum_{t=1}^{T} \left(E_t^{cha} + E_t^{dis} \right) + \eta_r^h \sum_{t=1}^{T} (H_t^{cha} + H_t^{dis}) \\ C_{cost} = C_S^E + C_S^{H_2} + C_S^h \end{cases} \tag{14}$$

Here, C_{ESS} is the total revenue of Energy Storage System (ESS); C_{in} and C_{cost} denote the operational revenue and investment cost of the ESS, respectively. η_r^e and η_r^h are the charging/discharging prices for electricity and thermal energy storage; E_t^{cha} and E_t^{dis} are the amounts of electricity charged to and discharged from the ESS. H_t^{cha} and H_t^{dis} are the corresponding thermal charge and discharge amounts; C_S^E , $C_S^{H_2}$ and C_S^h indicate the investment costs for electricity, hydrogen, and thermal energy storage, respectively.

3.2.2 Constraints

Energy storage devices store excess energy during periods of low load and high renewable energy generation. Their energy time-shifting characteristics can effectively alleviate supply-demand imbalances in the park and address the uncertainty of renewable energy output. The energy storage devices in the ESS include fuel cell storage, hydrogen storage tanks, and thermal storage tanks. While the models for different types of energy storage devices are similar in form, constraints such as capacity and charge/discharge power must be considered.

Fuel Cell Constraints:

The operating power and ramp-rate constraints of the fuel cell are given by:

 doi:10.20944/preprints202509.2162.v1

$$\begin{cases} S_t^E = S_{t-1}^E(1-\delta^E) + (P_t^{E,cha}\eta^{E,cha} - \dfrac{P_t^{E,dis}}{\eta^{E,dis}})\Delta t \\ S_{min}^E \le S_t^E \le S_{max}^E \\ 0 \le P_t^{E,cha} \le \omega_t^{E,cha} P_{max}^{E,cha} \\ 0 \le P_t^{E,dis} \le \omega_t^{E,dis} P_{max}^{E,dis} \\ 0 \le \omega_t^{E,cha} + \omega_t^{E,dis} \le 1 \\ S_{t=0}^E = S_{t=T}^E \end{cases} \tag{15}$$

where S_t^E, S_{min}^E and S_{max}^E represent the state-of-charge and its lower/upper limits for electrical storage at time t; $P_t^{E,cha}$, $P_t^{E,dis}$, $P_{max}^{E,cha}$ and $P_{max}^{E,dis}$ denote the charge/discharge power and their upper limits; δ^E is the self-discharge coefficient; $\eta^{E,cha}$ and $\eta^{E,dis}$ indicate charge/discharge efficiencies; $\omega_t^{E,cha}$ and $\omega_t^{E,dis}$ are binary variables representing charge/discharge states; $S_{t=0}^E$ and $S_{t=T}^E$ specify the initial and final states-of-charge.

8. Hydrogen-tank constraints:

The hydrogen storage level and charge/discharge rate constraints are formulated as:

$$\begin{cases} V_t^{H_2} = V_{t-1}^{H_2}(1-\delta^{H_2}) + (H_t^{H_2,cha}\eta^{H_2,cha} - \dfrac{H_t^{H_2,dis}}{\eta^{H_2,dis}})\Delta t \\ V_{min}^{H_2} \le V_t^{H_2} \le V_{max}^{H_2} \\ 0 \le V_t^{H_2,cha} \le \omega_t^{H_2,cha} V_{max}^{H_2,cha} \\ 0 \le V_t^{H_2,dis} \le \omega_t^{H_2,dis} V_{max}^{H_2,dis} \\ 0 \le \omega_t^{H_2,cha} + \omega_t^{H_2,dis} \le 1 \\ S_{t=0}^{H_2} = S_{t=T}^{H_2} \end{cases} \tag{16}$$

where $V_t^{H_2}$, $V_{min}^{H_2}$ and $V_{max}^{H_2}$ represent the hydrogen storage volume and its lower/upper limits for the hydrogen tank at time t; $V_t^{H_2,cha}$, $V_t^{H_2,dis}$, $V_{max}^{H_2,cha}$ and $V_{max}^{H_2,dis}$ denote the hydrogen charging/discharging rates and their upper limits; δ^{H_2} is the self-loss coefficient; $\eta^{H_2,cha}$ and $\eta^{H_2,dis}$ indicate the charging/discharging efficiencies; $\omega_t^{H_2,cha}$ and $\omega_t^{H_2,dis}$ are binary variables representing the charging/discharging states; $S_{t=0}^{H_2}$ and $S_{t=T}^{H_2}$ specify the initial and final hydrogen storage volumes over a scheduling cycle.

9. Thermal Storage Tank Constraints:

The thermal energy storage level and charge/discharge rate constraints are formulated as:

$$\begin{cases} H_t^{hot} = H_{t-1}^{hot}(1-\delta^{hot}) + (H_t^{hot,cha}\eta^{hot,cha} - \dfrac{H_t^{hot,dis}}{\eta^{hot,dis}})\Delta t \\ H_{min}^{hot} \le H_t^{hot} \le H_{max}^{hot} \\ 0 \le H_t^{hot,cha} \le \omega_t^{hot,cha} H_{max}^{hot,cha} \\ 0 \le H_t^{hot,dis} \le \omega_t^{hot,dis} H_{max}^{hot,dis} \\ 0 \le \omega_t^{hot,cha} + \omega_t^{hot,dis} \le 1 \\ S_{t=0}^{hot} = S_{t=T}^{hot} \end{cases} \tag{17}$$

where H_t^{hot}, H_{min}^{hot} and H_{max}^{hot} represent the hydrogen storage volume and its lower/upper limits for the hydrogen tank at time t; $H_t^{hot,cha}$, $H_t^{hot,dis}$, $H_{max}^{hot,cha}$ and $H_{max}^{hot,dis}$ denote the hydrogen charging/discharging rates and their upper limits; δ^{hot} is the self-loss coefficient; $\eta^{hot,cha}$ and $\eta^{hot,dis}$ indicate the charging/discharging efficiencies; $\omega_t^{hot,cha}$ and $\omega_t^{hot,dis}$ are binary variables representing the charging/discharging states; $S_{t=0}^{hot}$ and $S_{t=T}^{hot}$ specify the initial and final hydrogen storage volumes over a scheduling cycle.

4. Case Study

4.1 Scenario Design

Using operational data from a large-scale industrial park IES as an example, the scheduling cycle T is set to 24 hours. The forecasted output curves of renewable generation (wind and PV) and the electricity/heat load demand profiles are shown in Figure 4. The parameters of all equipment and models are presented in Table 1.

 doi:10.20944/preprints202509.2162.v1

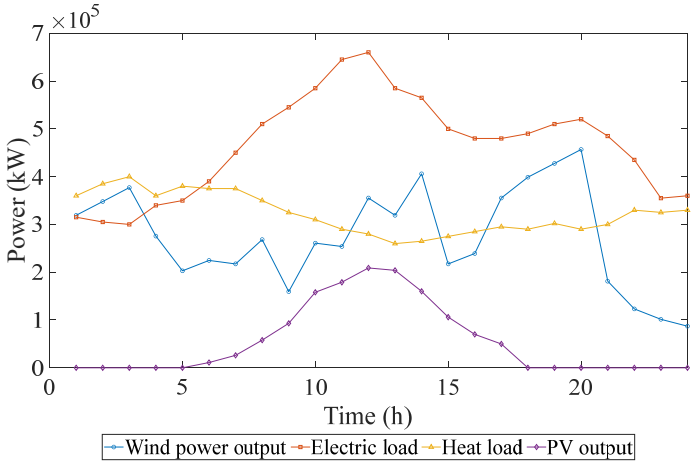

Figure 4. Load and wind/PV output forecast curves

Table 1. Equipment and model parameters.

Parameter type	Value	Parameter type	Value
Coal price	800 CNY/ton	Electric boiler	40MW
gas price	3.5 CNY/m³	Min/max output of thermal power unit	100/40MW
Electrical output per CHP unit	125MW	Ramping limits of the thermal power unit	80/-80 MW/h
Thermal output per CHP unit	150MW	Electrical storage capacity and power	50MWh/25MW
Gas boiler output	80MW	Thermal storage capacity and power	60MWh/15MW

This study establishes five comparative scenarios for analysis:

Scenario 1: Adopts the most basic IES model without considering DR, energy storage, or tiered carbon trading.

Scenario 2: Builds upon Scenario 1 by incorporating DR to specifically examine its load regulation effect.

Scenario 3: Extends Scenario 2 with a hybrid energy storage configuration, still under unified dispatch by the IES operator (i.e., non-independent storage entity), to verify the combined effect of DR and energy storage.

Scenario 4: Introduces tiered carbon trading based on Scenario 3, with energy storage remaining as a centralised ancillary resource of IES, jointly investigating the low-carbon and economic benefits under the tripartite interaction.

Scenario 5: Further develops Scenario 4 by designating energy storage as an independent operational entity and applying the proposed bi-level optimal method.

4.2 Analysis of IES Operating Costs

First, the operational costs of the IES under the aforementioned five scenarios are validated and comparatively analysed. The statistical results of operational costs are presented in Table 2.

Table 2. System operating cost results.

Scenario	Total cost/CNY	Coal consumption cost / CNY	Gas purchase cost / CNY	Electricity purchase cost/ CNY	Renewables utilisation rate

 doi:10.20944/preprints202509.2162.v1

1	4298067	975228800	4290926	7141	0.791
2	3419853	887642600	4301328	63211	0.834
3	3199424	781586964	4317435	0	0.929
4	4405988	867929814	4085194	0	0.95
5	3783769	995716800	3169273	0	1

As shown in Table 2, Scenario 1 exhibits the highest total operational cost at 4,298,100, with a renewable energy utilisation rate of 0.791. After introducing DR in Scenario 2, the total system cost decreases to ¥3,419,900 (a 20.4% reduction compared to Scenario 1), while the renewable utilisation rate improves from 0.791 to 0.834. This demonstrates DR's positive role in enhancing clean energy integration. Scenario 3 incorporates hybrid energy storage, further reducing operational costs to ¥3,199,400, highlighting the critical function of energy storage in coordinating electric/thermal load regulation and peak shaving. Renewable energy utilisation also becomes more efficient. Although Scenario 4 experiences a slight cost increase (¥4,406,000) due to explicit carbon emission pricing, the carbon-constrained mechanism promotes environmentally friendly dispatch. The renewable utilisation rate rises to 0.950, and overall system emissions are effectively suppressed. With the bi-level optimal mechanism introduced in Scenario 5, the total operational cost drops to ¥3,783,769 (a 14.1% reduction compared to Scenario 4). This cost reduction primarily stems from the independent operation of energy storage, which no longer solely serves IES objectives but instead optimises charging/discharging strategies flexibly: reducing reliance on external grid purchases and maximising profits through market-oriented dispatch.

However, despite the cost reduction in Scenario 5, the independent energy storage operator prioritises economic benefits over low-carbon operation in the absence of strict carbon constraints. Consequently, coal consumption costs increase, revealing a potential trade-off between economic and environmental objectives. Furthermore, the independent storage operator, free from external dispatch targets, can dynamically adjust charging/discharging based on electricity prices and renewable generation fluctuations. This autonomous scheduling eliminates renewable curtailment, achieving full utilisation (renewable rate = 1).

In summary, the proposed hybrid energy storage cooperative optimal method demonstrates superior performance in balancing economic efficiency and operational flexibility, while DR and energy storage significantly enhance renewable utilisation and system efficiency. Nevertheless, without carbon constraints, economic and environmental goals may conflict. Future dispatch strategies should better harmonise low-carbon objectives with economic viability to ensure sustainable development.

4.3 Analysis of Low-Carbon Benefits of the IES

To quantify the carbon emission control effects across different scenarios, Figure 5 presents the carbon emissions from major energy equipment, carbon capture volumes, and the total system carbon emissions under the five operational scenarios described above.

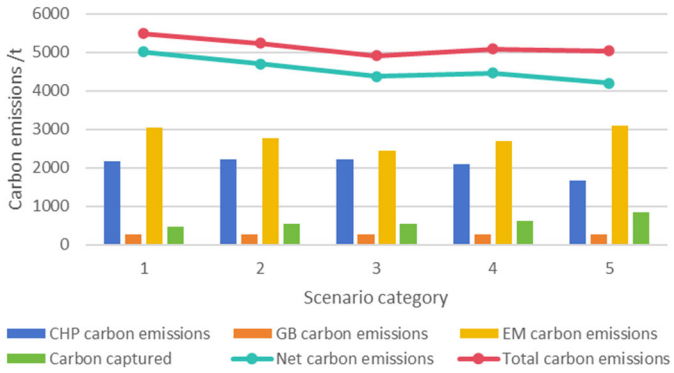

Figure 5. Carbon Emissions Data

 doi:10.20944/preprints202509.2162.v1

In Scenario 1, total carbon emissions reached 5,010.84 tons, with the lowest level of carbon capture at 483.27 tons. Upon the introduction of DR in Scenario 2, emissions declined to 4,700.41 tons, representing a reduction of approximately 6.2% compared to Scenario 1. Building upon this, Scenario 3 incorporates the role of energy storage, further decreasing emissions to 4,377.90 tons: a 12.6% reduction from the baseline. In Scenario 4, the inclusion of a tiered carbon pricing mechanism results in total emissions of 4,465.41 tons, while the carbon capture amount increases significantly to 618.53 tons.

Scenario 5 integrates multiple mechanisms: independent energy storage, bi-level optimisation, DR, CCS, and carbon trading, achieving a total system carbon emission of 4,206.49 tons, the lowest among all scenarios and approximately 804.35 tons (16.1%) lower than in Scenario 1. The carbon capture level in Scenario 5 also rises to 835.42 tons, the highest across all cases. This improvement is primarily attributed to the independent storage operator's price- and carbon-driven autonomous charge/discharge strategy, which, combined with DR reshaping the load curve, enables the substitution of high-carbon generation during periods of high marginal carbon cost. Furthermore, under carbon pricing constraints, the marginal benefits of low-carbon technologies are amplified, thereby achieving the dual low-carbon objective of "lowest emissions + highest carbon capture."

These findings highlight that Scenario 5 demonstrates the synergistic advantages of multi-mechanism integration and market-based energy storage operation, positioning it as the most carbon-effective configuration among all the examined cases.

4.4 Benefit Analysis of Independently Operated Hybrid Storage

The economic contribution of energy storage systems to integrated energy systems varies under different optimal dispatch methods. Therefore, we have conducted a statistical analysis of the total costs, total revenues, and net benefits of electricity, heat, and hydrogen storage systems for Scenarios 3 to 5. The results are presented in Table 3:

Table 3. Storage Benefit Analysis.

Scenario	Total storage cost /CNY	Total storage revenue /CNY	Net revenue /CNY
3	30809.45	204133.25	173323.80
4	28587.59	198658.63	170071.04
5	190342.40	527587.60	337245.20

According to the results in Table 3, the benefits of energy storage in Scenario 3 and Scenario 4 are relatively similar, with both demonstrating significantly higher storage revenues compared to their corresponding costs. In Scenario 4, after the introduction of the carbon trading mechanism, the carbon emission constraints partially limited the system's dispatch flexibility, resulting in a reduced marginal contribution from energy storage. Consequently, the net profit declined to ¥170,071.04. Nevertheless, Scenario 4 outperformed in terms of carbon capture (618.53 tons) and system-wide carbon emission reduction (4,465.41 tons). This indicates that, under multi-objective dispatch, energy storage can sacrifice part of its economic gains in exchange for improved low-carbon system performance. It is an outcome that reflects a trade-off optimal strategy of "environmental benefit over profit".

In Scenario 5, energy storage is upgraded from a system-dependent asset to an independent market participant. Although the initial investment and the scale of installation and operation were considerably increased, raising the total storage cost to ¥190,342.40, the revenues still significantly outweighed the costs. This was achieved by improving local utilisation of renewable energy, enhancing system flexibility, reducing carbon emissions, and leveraging electricity price arbitrage. The net profit in this scenario reached ¥337,245.20. The core advantage lies in the bi-level optimal framework, which grants energy storage greater autonomy in scheduling and arbitrage, thereby achieving a synergistic benefit of "enhanced economic efficiency + optimal clean energy integration." On one hand, the system's reliance on high-carbon energy sources such as coal and natural gas is

 doi:10.20944/preprints202509.2162.v1

reduced, significantly lowering emissions; on the other, the increased flexibility enhances system stability and the ability to accommodate renewable generation fluctuations under high renewable penetration levels. These results robustly demonstrate the comprehensive economic and environmental value of independent energy storage systems.

Figure 6-Figure 11 provide a comparative analysis of the benefits associated with electricity, thermal, and hydrogen storage. EES clearly reflects the "low-price charging and high-price discharging" arbitrage mechanism. Scenarios 3 and 4 show higher unit economic efficiency, with Scenario 4 offering improved benefit-cost ratios and return on investment under carbon constraints. In Scenario 5, although electricity storage as an independent operator generates higher absolute net profits, investment and operational costs also increase accordingly.

In comparison, thermal energy storage yields lower direct returns than electrical storage but exhibits significant system-level synergistic value. It flattens thermal loads and stabilises CHP operation by shifting heat supply from off-peak to peak periods, thus alleviating the output pressure on GBs. In Scenario 4, carbon constraints further magnify the positive effects of electric-thermal coupling. In Scenario 5, in conjunction with electrical storage, power-to-heat conversion becomes more seamless; however, the expansion in scale leads to a marginal decline in unit efficiency.

Hydrogen storage demonstrates a threefold value: renewable absorption, energy conversion, and low-carbon benefits. It absorbs excess electricity during low-price or curtailed periods through hydrogen production, achieving energy vector transformation and generating terminal value via external sales or process substitution. Additionally, replacing carbon-based fuels with hydrogen contributes directly to emission reductions. In Scenario 5, the independence and scaling-up of hydrogen storage further enhance its arbitrage and low-carbon benefits, significantly improving the local utilisation of renewables and the temporal matching between generation and load.

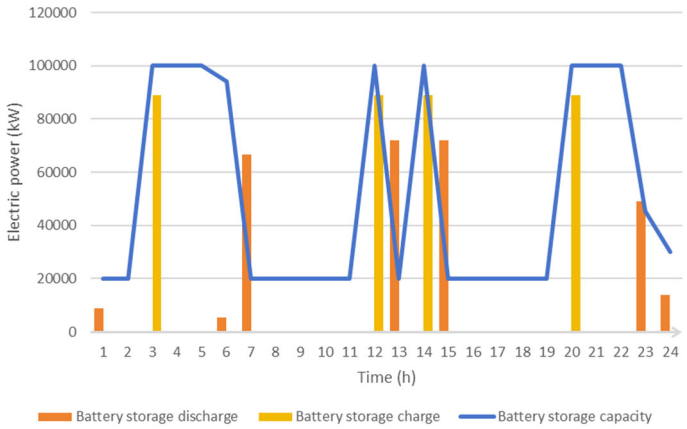

Figure 6. Electrical battery storage optimal scheduling results

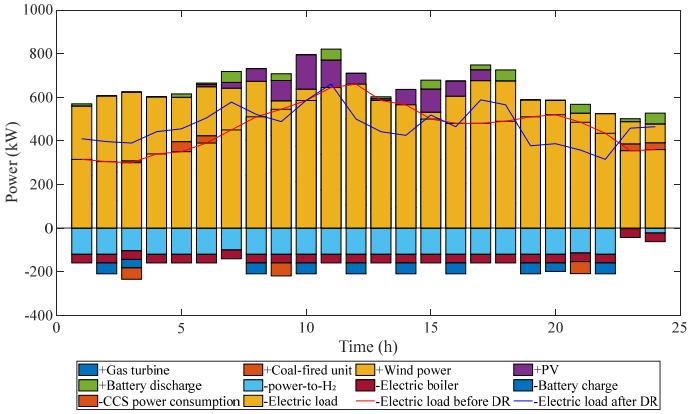

 doi:10.20944/preprints202509.2162.v1

Figure 7. Electric power balance diagram

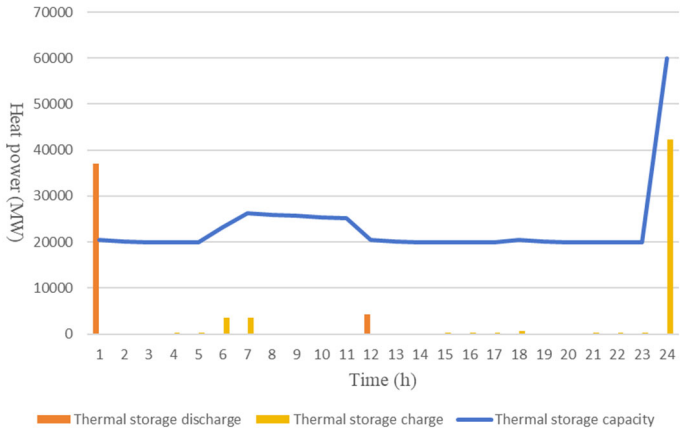

Figure 8. Thermal storage optimal scheduling results

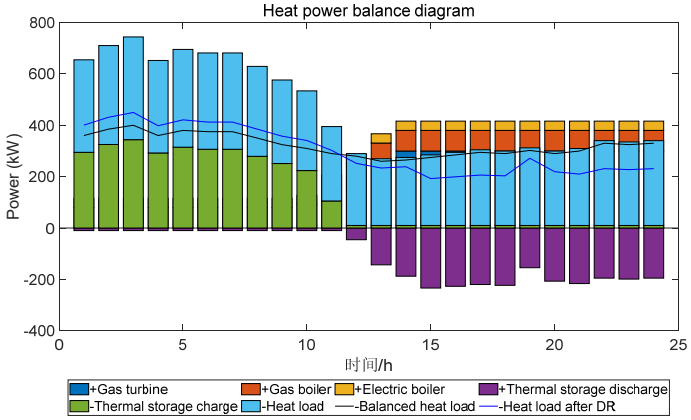

Figure 9. Heat power balance diagram

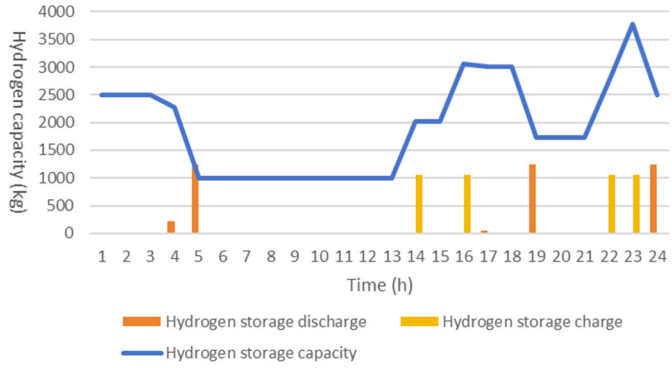

Figure 10. Hydrogen storage optimal scheduling results

 doi:10.20944/preprints202509.2162.v1

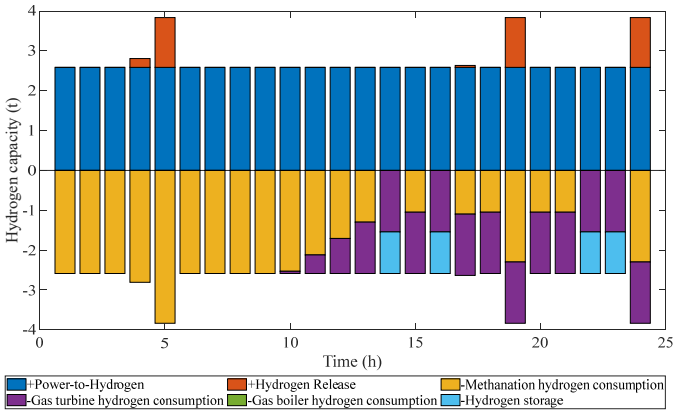

Figure 11. Hydrogen Power Balance Diagram

5. Conclusion

This study addresses the inherent trade-offs among low-carbon operation, economic efficiency, and system flexibility within IES, and proposes a Stackelberg bi-level optimal model in which energy storage is scheduled independently by a third-party operator. The primary innovations of the model are reflected in the following aspects:

(1) Methodological Innovation: The model breaks away from the traditional centralised storage dispatch paradigm by integrating multiple types of energy storage under an independent operator framework. This approach significantly enhances the dispatchability and marketability of ESS within coupled energy networks.

(2) Structural Incentive Design: Through upper-lower level game-theoretic coordination, energy storage simultaneously serves the IES-level system objectives while maintaining its own arbitrage capability in response to price signals such as electricity price, carbon price, and DR. This forms an incentive-compatible structure that aligns system-level optimality with individual-level profitability.

(3) Performance Outcomes: Case studies demonstrate that independently optimised energy storage scheduling not only reduces IES operational costs and carbon emissions but also improves renewable energy utilisation and increases net storage revenue. It thereby offers a viable pathway toward dynamically balancing economic performance and low-carbon objectives, while enhancing system-level operational flexibility.

Acknowledgments: This work is based on the Science and Technology Project of State Grid Jiangsu Electric Power Co., Ltd. Electric Power Research Institute (J2024JC-04).

Data availability: The relevant data of calculation used to support the findings of this study are included within the article.

Abbreviations

The following abbreviations are used in this manuscript:

CCS	Carbon Capture and Storage
CHP	Combined Heat and Power
EBs	Electric Boilers
EES	Electrical Energy Storage
GBs	Gas Boilers
HES	Hydrogen Energy Storage
IES	Integrated Energy Systems
P2G	Power-to-Gas
TPUs	Thermal Power Units

 doi:10.20944/preprints202509.2162.v1

References

1. Liu, J.; Ma, L.; Wang, Q. Energy Management Method of Integrated Energy System Based on Collaborative Optimization of Distributed Flexible Resources. *Energy* **2023**, *264*, 12598.
2. Xiong, Z.; Zhang, D.; Wang, Y. Optimal Operation of Integrated Energy Systems Considering Energy Trading and Integrated Demand Response. *Energy Reports* **2024**, *11*, 3307–331.
3. Yang, C.; Dong, X.; Wang, G.; Lv, D.; Gu, R.; Lei, Y. Low-Carbon Economic Dispatch of Integrated Energy System with CCS-P2G-CHP. *Energy Reports* **2024**, *12*, 42–5.
4. Jiang, H.; Liu, X.; Zhou, H.; Zhao, Y.; Yao, Z. Multi-Time-Scale Optimal Scheduling Strategy of Electricity-Heat-Cold-Gas Integrated Energy System Considering Ladder Carbon Trading. *Energy Reports* **2025**, *13*, 4000–401.
5. Hannan, M.A.; Faisal, M.; Jern Ker, P.; Begum, R.A.; Dong, Z.Y.; Zhang, C. Review of Optimal Methods and Algorithms for Sizing Energy Storage Systems to Achieve Decarbonization in Microgrid Applications. *Renewable and Sustainable Energy Reviews* **2020**, *131*, 110022.
6. Hu, Y.; Yang, B.; Wu, P.; Wang, X.; Li, J.; Huang, Y.; Su, R.; He, G.; Yang, J.; Su, S.; et al. Optimal Planning of Electric-Heating Integrated Energy System in Low-Carbon Park with Energy Storage System. *Journal of Energy Storage* **2024**, *99*, 113327.
7. Guo, J.; Liu, Z.; Li, Y.; Wu, D.; Liu, X.; Zhang, S.; Yang, X.; Ge, H.; Zhang, P. Thermodynamic Performance Analyses and Optimization Design Method of a Novel Distributed Energy System Coupled with Hybrid-Energy Storage. *Renewable Energy* **2022**, *182*, 1182–120.
8. Khan, T.; Yu, M.; Waseem, M. Review on Recent Optimization Strategies for Hybrid Renewable Energy System with Hydrogen Technologies: State of the Art, Trends and Future Directions. *International Journal of Hydrogen Energy* **2022**, *47*, 25155–2520.
9. Fukaume, S.; Nagasaki, Y.; Tsuda, M. Stable Power Supply of an Independent Power Source for a Remote Island Using a Hybrid Energy Storage System Composed of Electric and Hydrogen Energy Storage Systems. *International Journal of Hydrogen Energy* **2022**, *47*, 13887–1389.
10. Zhou, J.; Li, S.; Zhou, X.; Li, C.; Xiong, Z.; Zhao, Y.; Liang, G. Operation Optimization for Gas-Electric Integrated Energy System with Hydrogen Storage Module. *International Journal of Hydrogen Energy* **2022**, *47*, 36622–36639.
11. Li, L.; Sun, Y.; Han, Y.; Chen, W. Seasonal Hydrogen Energy Storage Sizing: Two-Stage Economic-Safety Optimization for Integrated Energy Systems in Northwest China. *iScience* **2024**, *27*, 11069.
12. Zhang, W.; Maleki, A.; Rosen, M.A.; Liu, J. Optimization with a Simulated Annealing Algorithm of a Hybrid System for Renewable Energy Including Battery and Hydrogen Storage. *Energy* **2018**, *163*, 191–20.
13. Yan, Z.; Zhang, Y.; Liang, R.; Jin, W. An Allocative Method of Hybrid Electrical and Thermal Energy Storage Capacity for Load Shifting Based on Seasonal Difference in District Energy Planning. *Energy* **2020**, *207*, 11813.
14. Li, J.; Chen, H.; Li, J.; Zhang, Y.; Pan, P.; Bian, J.; Yu, Z. Bi-Level Optimization Model of Hydrogen-Blended Gas Units and Multi-Type Energy Storage System Considering Low-Carbon Operation. *Energy* **2025**, *314*, 13416.
15. Li, Y.; Hu, W.; Zhang, F.; Li, Y. Collaborative Operational Model for Shared Hydrogen Energy Storage and Park Cluster: A Multiple Values Assessment. *Journal of Energy Storage* **2024**, *82*, 110507.
16. Chen, N.; Gao, J.; Gao, L.; Yang, S.; Chen, S. Scheduling Strategy for an Electricity-Heat-Gas Hybrid Energy Storage Microgrid System Considering Novel Combined Heat and Power Units. *Energy Reports* **2025**, *13*, 4719–473.
17. Zhang, B.; Xia, Y.; Peng, X. Robust Optimal Dispatch Strategy of Integrated Energy System Considering CHP-P2G-CCS. *Global Energy Interconnection* **2024**, *7*, 14–2.
18. Yang, C.; Dong, X.; Wang, G.; Lv, D.; Gu, R.; Lei, Y. Low-Carbon Economic Dispatch of Integrated Energy System with CCS-P2G-CHP. *Energy Reports* **2024**, *12*, 42–51.
19. Pan, C.; Jin, T.; Li, N.; Wang, G.; Hou, X.; Gu, Y. Multi-Objective and Two-Stage Optimization Study of Integrated Energy Systems Considering P2G and Integrated Demand Responses. *Energy* **2023**, *270*, 12684.

 doi:10.20944/preprints202509.2162.v1